Applied Geochemistry 23 (2008) 3059–3071

Contents lists available at ScienceDirect

Applied Geochemistry

journal homepage: www.elsevier.com/locate/apgeochem

Integrated biogeochemical and hydrologic processes driving arsenic release from shallow sediments to groundwaters of the Mekong delta

Benjamin D. Kocar [a], Matthew L. Polizzotto [a], Shawn G. Benner [b], Samantha C. Ying [a], Mengieng Ung [c], Kagna Ouch [c], Sopheap Samreth [c], Bunseang Suy [c], Kongkea Phan [c], Michael Sampson [c], Scott Fendorf [a,*]

[a] Department of Geological and Environmental Sciences, Stanford University, Stanford, CA 94305, USA
[b] Department of Geology, Boise State University, Boise, ID 83705, USA
[c] Resource Development International, Kien Svay, Kandal, Cambodia

ARTICLE INFO

Article history:
Available online 15 July 2008

ABSTRACT

Arsenic is contaminating the groundwater of Holocene aquifers throughout South and Southeast Asia. To examine the biogeochemical and hydrological processes influencing dissolved concentrations and transport of As within soils/sediments in the Mekong River delta, a ~50 km^2 field site was established near Phnom Penh, Cambodia, where aqueous As concentrations are dangerously high and where groundwater retrieval for irrigation is minimal. Dissolved As concentrations vary spatially, ranging up to 1300 μg/L in aquifer groundwater and up to 600 μg/L in surficial clay pore water. Groundwaters with high As concentrations are reducing with negligible dissolved O_2 and high concentrations of Fe(II), NH_4^+, and dissolved organic C. Within near-surface environments, these conditions are most pronounced in sediments underlying permanent wetlands, often found within oxbow channels near the Mekong River. There, labile C, co-deposited with As-bearing Fe (hydr)oxides under reducing conditions, drives the reductive mobilization (inclusive of Fe and As reduction) of As. Here, conditions are described under which As is mobilized from these sediments, and near-surface As release is linked to aquifer contamination over long time periods (100s to 1000s of years). Site biogeochemistry is coupled with extensive hydrologic measurements, and, accordingly, a comprehensive interpretation of spatial As release and transport within a calibrated hydraulic flow-field is provided of an As-contaminated aquifer that is representative of those found throughout South and Southeast Asia.

1. Introduction

Himalayan-derived As is contaminating groundwater within Asia, leading to tens of millions of individuals exposed to drinking water with hazardous levels of this metalloid (Ahmed et al., 2006; Nordstrom, 2002; Yu et al., 2003). The majority of affected people live in rural Bangladesh and West Bengal, India where, in an effort to minimize the incidences of surface water-borne diseases, hand-pumped tubewells have been in place since the 1960s (Chakraborti et al., 2002). Research on the fate and transport, as well as the health effects, of As have accordingly focused on areas of the Ganges–Brahmaputra–Meghna River system (Akai et al., 2004; Anawar et al., 2003; Dowling et al., 2002; Harvey et al., 2002; Islam et al., 2004; Nickson et al., 1998; van Geen et al., 2003). However, more recently, the occurrence of As in aquifers of the Mekong (Berg et al., 2007; Buschmann et al., 2007; Polya et al., 2003, 2005; Stanger et al., 2005) and Red River (Berg et al., 2001, 2007; Postma et al., 2007) systems has come to light. Similar to Bangladesh and West Bengal, high As concentrations are found in association with reducing, carbonate-dominated groundwaters. Moreover, each of the delta

* Corresponding author. Tel.: +650 723 5238; fax: +650 725 2199.
E-mail address: fendorf@stanford.edu (S. Fendorf).

0883-2927/$ - see front matter © 2008 Published by Elsevier Ltd.
doi:10.1016/j.apgeochem.2008.06.026

systems possess fine sediments transported from the Himalayas to flat, low-lying alluvial basins (Berg et al., 2001; JICA, 2002; Kinniburgh and Smedley, 2001) with underlying aquifer sands; thus similarities in geologic deposition, aquifer source rock, and regional hydrological gradients suggest that common processes may control As within the groundwater. Irrigation with groundwater is ubiquitous in the Ganges–Brahmaputra–Meghna basin, but within the Mekong Delta, particularly in Cambodia, limited groundwater pumping has occurred – even domestic wells have only been installed within the past decade. Thus, biogeochemical processes conducive to As release within the sediments may be examined within a relatively unperturbed hydrologic system. In a companion article (Benner et al., 2008), these hydrologic conditions are examined more thoroughly, providing a framework linking groundwater flow with the biogeochemical processes presented here.

A variety of biogeochemical processes may result in As release from solids to pore-water; As desorption/dissolution is generally considered to be mediated by ligand exchange reactions, reduction–oxidation (redox) processes, and dissolution of As-bearing solid phases (Smedley and Kinniburgh, 2002). However, release of As during the onset of reducing conditions and ensuing reductive dissolution of As-bearing Fe (hydr)oxides is generally ascribed as the dominant means of displacement from the solid phase (Ahmed et al., 2004; deLemos et al., 2006; McArthur et al., 2001). This hypothesis is supported by correlations between As and oxalate (solid phase) extractable Fe(III) in the aquifer sediments, as well as correlations between Fe(II) and soluble As in well waters (Ahmed et al., 2004; McArthur et al., 2001).

Although the biogeochemical processes influencing As partitioning are becoming increasingly well defined, the source(es) of As within South and Southeast Asian sediments are confounded by the spatial patterns of release. Numerous field and laboratory studies have suggested that the reductive dissolution of Fe (hydr)oxides within the deep aquifer may release As (Islam et al., 2004; McArthur et al., 2004); these claims are based on the presence of Fe-reducing organisms, subsurface peat (which fuels reductive dissolution of Fe (hydr)oxides), and generally reducing conditions. However, the presence of labile Fe (hydr)oxides within the aquifer is unresolved, and other studies contend that As is derived from biogeochemical processes occurring at or near the surface (Harvey et al., 2006; Polizzotto et al., 2005).

In an expansive study, Polizzotto et al. (2008) reveal steep vertical As gradients between surface sediments and the aquifer; with hydrologic measurements and As mass balance calculations they illustrate that release occurs within the near-surface sediments. Here the biogeochemical conditions conducive to and processes resulting in As release are examined within the Kandal province, Cambodia, where As concentrations in groundwater are as high as 100 times the World Health Organization recommended guideline of 10 μg/L (Buschmann et al., 2007; JICA, 2002; Polya et al., 2005). Detailed spatial As data within the soil/sediment/aquifer profile are presented and high As concentrations within the near-surface are linked to underlying aquifer contamination. Sediment collection, groundwater, surface water and hydraulic measurements were performed to examine spatial variations in pore-water As concentrations, solid-phase As concentrations, general aqueous chemistry, and hydraulic gradients spanning a large (>50 km^2) field area as well as two smaller, focused study areas. The results provide a novel dataset describing aqueous and solid-phase As within a representative As-rich Asian floodplain and a robust interpretation of changing As biogeochemistry as a function of time (100s to 1000s of years) is derived. Through integrating the biogeochemistry processes with a highly constrained hydrologic flow model of the upper Mekong Delta (Benner et al., 2008), the spatiotemporal pattern of As sources and sinks to pore-water within the aquifer system are revealed.

2. Field area

The massive deltas of Asia, inclusive of the Mekong and Ganges–Brahmaputra systems that drain the Himalayan uplift, quickly expanded following the cessation of rapid sea level rise ~7 ka ago. Each system has characteristic inverted and subdued deltaic topography, and associated hydrology is strongly influenced by the monsoonal-driven rise and fall of its respective rivers. The Mekong River is a broad river that carries the seventh largest sediment load in the world, the majority of which is discharged during the wet season. The delta floodplain is roughly 62,500 km^2 (Nguyen et al., 2000) and the upper 7–20 m of sediment has been deposited as a prograding deltaic sequence in the past 6–7 ka (Ta et al., 2002; Tamura et al., 2007) following the most recent sea level high stand. Below surficial overbank clays, Holocene sediments representing delta progradation include silts, sands and clays; gray sandy sediments encompass the majority of wells within the field area and are those with which high dissolved As concentrations are typically associated.

The field area in the Kandal province of Cambodia comprises approximately 50 km^2 between the Mekong and Bassac Rivers and is typical of the Mekong floodplain system. The region is characterized by elevated levees along river banks receding to a native wetland basin between the two rivers. The primary water-producing fine gray sand aquifer at the field site typically extends >50 m in depth and is overlain by a 3–20 m thick red and gray clay unit (Fig. 1a). A network of 80 installed wells and 10 surface water monitoring sites are distributed throughout the field area, and two focused study areas include near-surface lysimeters and a subset of closely spaced wells for more detailed spatial analyses (Fig. 1b).

3. Materials and methods

3.1. Well and lysimeter installation and aqueous sampling

3.1.1. Multi-depth well nests and tension lysimeters

Installation of wells was achieved using manual rotation of a 3.8 cm diameter pipe with a 10.2 cm cutting auger; water was continuously pumped through the pipe to

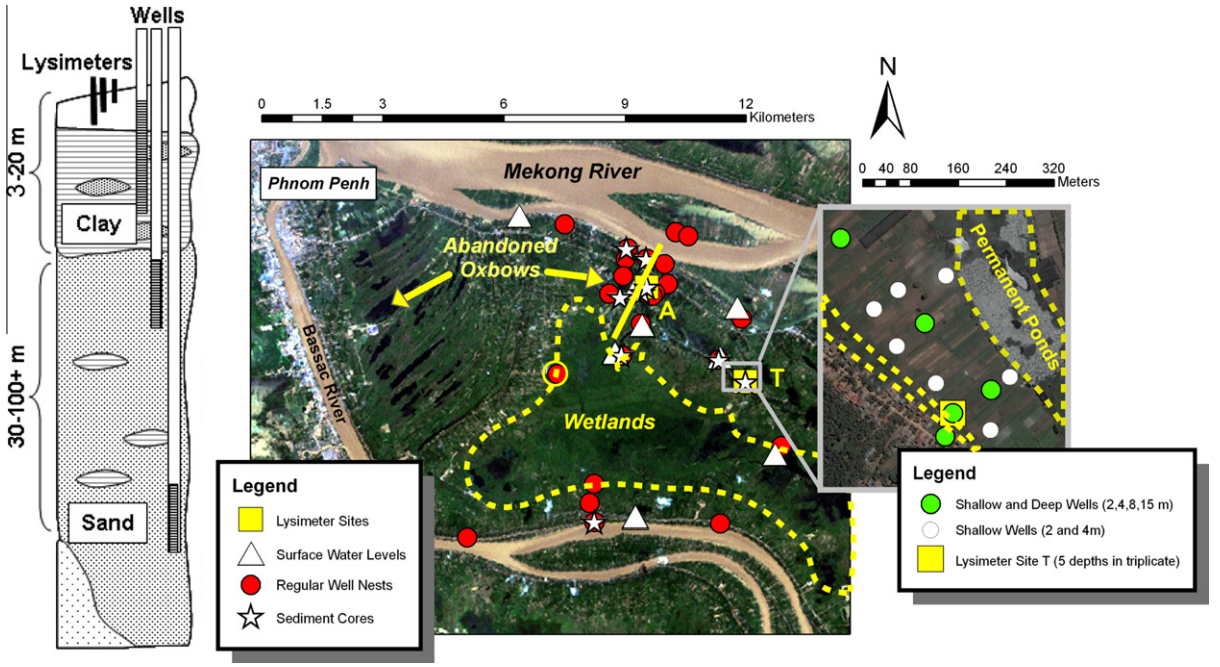

Fig. 1. (A) (left). Schematic illustration of sediment profile and location of tension lysimeters and wells. (B) (right). The field area is located ~20 km SE of Phnom Penh, Cambodia, situated in the Upper Mekong Delta. Wells were installed in transects from the Mekong River to the Bassac River; each red well symbol represents 3–6 wells screened at varying depths. The yellow dotted line shows the aerial extent of the central wetlands, and abandoned river channel oxbow ponds are indicated. Basemap is derived from LandSat images obtained from the University of Maryland Land Cover Facility (GLCF, 2005). The yellow line extending from SW to NE represents a transect of wells used in Fig. 2. Sediments and water from Sites A and T, and from a pit near well nest outlined in yellow (near left center of wetlands) were used to date sediments and DIC (Table 1). The blowup illustrates the detailed study area within an abandoned oxbow channel. (For interpretation of the references in color in this figure legend, the reader is referred to the web version of this article.)

physically displace sediment cuttings. Sections of pipe were progressively added to achieve the desired well depth (up to 60 m), and 3.2 cm PVC (with varying lengths of discreet screening) was inserted as well casing. Shallow (8–12 m depth) wells were installed with a 6 to 8 m screened interval, while medium (20–30 m) and deep wells (36–60 m) were constructed with screened intervals of 4 m. At each location, at least one shallow, medium and deep well was installed; 3–6 total wells were installed at each location. Wells were backfilled with coarse sand and capped with clay and/or cement.

Additional subsets of well nests were installed directly within an oxbow channel and were 2, 4 and 8 m deep. In these wells, shorter screened intervals (2 m) were used to examine groundwater from more discreet depths within the sediment profile. Each well depth was installed at four locations within the oxbow, while seven nests were installed with 2 and 4 m wells (Fig. 1b, blowup), which were dug with a bucket auger. Samples were collected at regular intervals from hand-augered holes for determination of total solid-phase As.

In order to monitor near-surface pore-water chemistry at specific depths within oxbow ponds, tension lysimeters (Prenart Equipment ApS, Denmark) were installed at two locations, denoted site A and site T (Fig. 1b). At site A, one lysimeter was installed at each depth of 0.1, 0.5, 1, 2 and 4 m, while three lysimeters were installed at these depths at site T (separated horizontally by at least 1.5 m). Holes were dug with a hand auger, sediments were saved in a bucket, and lysimeters were installed. Boreholes were then backfilled and sealed with the original sediments. Sites A and T possess similar sedimentary characteristics and are both located within the confines of an oxbow channel (identified with satellite imagery and field observations). They are characterized by 1–3 m of orange sediments overlying a transition to gray clay. Fine sands are encountered ~12 m below the surface.

3.1.2. Well, lysimeter, and surface water collection

A peristaltic pump (Geopump II, Geotech Environmental Equipment, Inc) was used to draw well water at a rate of ~1 L/min into a flow cell (YSI Inc, Ohio, USA) housing a YSI 556 multiparameter probe. Temperature, Eh, pH, conductivity and dissolved O_2 (DO) were continuously measured and recorded upon stabilization, which typically occurred within 10–130 min. Low yield wells were pumped dry and re-infiltrated water was collected on the following day.

Upon DO stabilization, groundwater samples were filtered through a 0.45 μm filter into acid washed bottles. Samples taken for cation and As measurement were acidified with trace metal grade HCl, while samples taken for anion analysis were pretreated with Bio-Rad AG50W-X8 cation exchange resin to eliminate metals from solution, which could precipitate and scavenge anions. Samples for analysis of dissolved organic C (DOC), NO_3^- and NH_4 samples were acidified with HCl, and $HgCl_2$ was also added to insure sterility (Wolf et al., 1989). Most wells were

sampled once during the wet season and once during the dry season. A subset of wells existing on a transect perpendicular to the Mekong River was sampled monthly.

Lysimeters were allowed to equilibrate with porewater for 30 d; during this time, several samples were collected and discarded. Each lysimeter at site A was subsequently sampled at least every month from August 2005–Sept 2007, and Site T lysimeters were sampled every month from July 06 to Sept 07. Porewater was drawn by suction (−800 mBar) into bottles, each containing 15 mL of Trace-Metal grade 3M HCl.

Surface water was collected on a monthly basis at the water–air interface. Sample treatment was identical to the groundwater samples.

3.2. Aqueous chemical analysis

Arsenic was measured with hydride generation inductively coupled plasma atomic emission spectroscopy (HG-ICP-AES). Briefly, 1 mL of 5% KI in 12 M HCl was added to 3 mL of sample to pre-reduce As(V) to As(III). Arsine gas was generated by addition of 0.5% $NaBH_4$/0.5% NaOH and quantified with HG-ICP-AES (Masscheleyn et al., 1991); the detection limit using this method was 5 μg/L.

Aluminum, Ca, K, Fe, Mg, Mn, Na, P, S and Si were measured by ICP-AES, and quality control standards were monitored throughout the course of the analysis. Anions, including F^-, Cl^-, NO_3^-, PO_4^{3-} and SO_4^{2-} were analyzed with a Dionex 500DX ion chromatograph using an AS9 guard/high capacity column, with a flow rate of 1.0 mL/min and using a 9 mM Na_2CO_3 isocratic eluent.

Dissolved organic C (DOC) was quantified as non-purgeable organic C on a Shimadzu TOC-5000A analyzer (Shimadzu Corporation, Japan). After acidification, sparging with N_2, and combustion, DOC was measured with a non-dispersive infrared gas analyzer. Carbon-14 measurements of dissolved inorganic C were performed at the University of Waterloo Environmental Isotopes Laboratory.

Field measurements on aqueous samples were performed to quantify As, alkalinity, Fe^{2+}, NO_3^-, SO_4^{2-} and sulfide. All measurements, with the exception of alkalinity and sulfide, were repeated in the laboratory. Alkalinity was determined by titrating the sample with 1.6 M H_2SO_4 to a colorimetric endpoint using a Hach digital titrator and bromocrescol green-methyl red indicator (Hach). Sulfide was measured with a DR 2400 Portable Spectrophotometer (Hach) using defined protocols. Nitrate and NH_4^+ were measured in the laboratory with an Alpkem Continuous-Flow Analyzer (OI Corporation, Texas, USA).

3.3. Solid-phase collection and analysis

3.3.1. Intact core collection

Intact cores were collected from aquifer and near-surface (<4 m) environments. Intact cores from the aquifer were obtained by driving a 1.9 cm open core device (AMS, Idaho, USA) fitted with a polycarbonate sleeve and core catcher into undisturbed sediments during the well drilling process. Near-surface cores were collected with an AMS soil sampling device fitted with a slide hammer and 5 cm × 15.2 cm core sampler containing a polycarbonate sleeve. Cores were collected at regular intervals (~25 cm) near installed lysimeters to a depth of 4 m. Aquifer cores were collected at several locations (Fig. 1b). All intact core samples were placed in gas-tight bags with a Mitsubishi Anaeropack to maintain anaerobic conditions. Cores were refrigerated and transported/stored at 4 °C until analysis. An additional subset of cores was collected from a 16 m deep, freshly dug open pit for C dating; approximately 20 cm of the pit wall was carefully removed to reveal a fresh surface, and 0.5 m of clean Cu pipe was pounded horizontally into the sediments. The pipes were then removed, and the ends sealed with paraffin wax and refrigerated. Upon return to the laboratory, the paraffin was carefully removed and the core contents sent to the NSF-Arizona AMS Laboratory (University of Arizona) for ^{14}C dating.

3.3.2. Total digestion and selective extractions

Total digestions were performed on intact core samples and samples collected during hand-augering. Samples were first homogenized in an anaerobic polyethylene glovebag with a mortar and pestle, and passed through a 200 μm sieve to remove plant roots and miscellaneous debris. A small amount of sample, 0.1 g, was microwave digested following US EPA protocol 3052 (3:1 concentrated HNO_3:concentrated HF). The digested sediments were then evaporated, reconstituted in HCl, and measured by ICP-AES or HG-ICP-AES (for As) as described above. The detection limit for HG-ICP-AES is 5 μg/L; thus, the detection limit for As within 0.1 g solid phase was 0.5 mg/kg, based on a total digestion volume of 10 mL.

Intact cores were dried under anaerobic conditions, homogenized, sieved, and subjected to selective chemical extractions similar to Keon et al. (2001) to determine different pools of As. However, extractions were performed in parallel (rather than in a series) to avoid possible chemical artifacts induced by sequential treatments. Sediments were treated with different chemicals to target water displaceable, salt exchangeable (1 M $MgCl_2$), ligand displaceable (1M PO_4^{2-}, pH 5.0), acid digestible (1 M HCl nominally for AVS/carbonates/amorphous oxides), and reducible metal (Fe and Mn) oxides (citrate–bicarbonate–dithionate extraction) (Loeppert and Inskeep, 1996). Extracts were analyzed with HG-ICP-AES and ICP-AES as mentioned above.

3.3.3. Synchrotron analysis

Arsenic-mineral associations, oxidation state and coordination environment were examined using X-ray fluorescence (XRF) spectroscopy and X-ray adsorption spectroscopy (XAS) at the undulator beamline 13-ID-C, Advance Photon Source (APS), Argonne National Laboratory. The storage ring operated at 7 GeV, and current was maintained at 100 mA via periodic electron injection. Energy selection was achieved with a Si(1 1 1) monochrometer. Samples were prepared by spreading sediment on a polycarbonate holder, and sealing the holder with gas-impermeable Kapton tape. Samples were rastered in 5 μm increments around a 5 × 5 μm X-ray beam and fluorescent X-rays were measured with a 16-element solid-state

energy-dispersive Ge detector. Incident and transmitted X-ray intensities were measured using in-line ionization chambers. Multiple X-ray fluorescent maps were made on sediments from each depth, and areas of high As concentration were analyzed with micro-X-ray absorption near-edge structure (μ-XANES) spectroscopy to determine As speciation. Sample spectra were collected from 50 to 100 eV above the As Kα edge of 11867 eV, and speciation was determined through a spectral analysis of first derivative peaks from the XANES spectra of As standards.

3.4. Hydrological measurements

The hydrology of the site, including methodology, is described in detail within the accompanying companion article (Benner et al., 2008). Briefly, wells, surface water points and Mekong River Phnom Penh Port (upstream of the site) and the Neak Leung (downstream) stations were surveyed, with the latter two points providing a reference datum for hydrologic measurements. Hydraulic heads and surface water levels were measured weekly from a fixed height. Hydraulic conductivities were determined from both aquifer sands and overlying clay layers using constant head permeameter tests and particle size analysis in the laboratory and slug tests in the field.

4. Results

4.1. Field-wide sedimentary and groundwater profiles

4.1.1. Sedimentary profile

Orange and gray clay levee/overbank deposits, often containing abundant wood and organic material representing historic mangrove swamp and coastline (6–8 ka), overlay the aquifer comprised of fine gray sand. Clay deposits are thickest (>20 m) in natural levees adjacent to oxbow channels and the Mekong and Bassac Rivers, but are often relatively thin within the confines of the oxbows (3–15 m), where variably-saturated wetlands dominate the landscape; such is the case at sites A and T, where the clay/silt transition to sand occurred at ~12 m below ground. Gray sands typically persist from below the overbank deposits to depths greater than 60 m, the depth of the deepest wells. Solid-phase As concentrations are highest in shallow, clayey sediments (12 mg/kg), derived from recent (<6–7 ka) floodplain deposits, while deeper gray sandy sediments (>~7 m, >~7.0 ka, Tamura et al., 2007) have relatively lower concentrations (2 mg/kg). Hydraulic measurements (Benner et al., issue) and resulting estimates of travel times from wetland environments to the Mekong River suggest residence times of 200–1000 a. These estimates of travel time coupled with ^{14}C dating of sediments (which are greater than 6 ka within the aquifer, Table 1) within the field site indicate that the aquifer has been flushed with multiple pore volumes, which has purged remnant saltwater and/or initially released As over the lifetime of the aquifer. Present As concentrations therefore, must result due to release from more recent near-surface sediments or continued release from older, buried sediments (see Section 5).

Table 1
Radiocarbon dates of sediments, wood and DIC

Location	Depth (m)	Material	^{14}C age BP (a)	Corrected Age BP (a)[a]
Site T	0.1	Sediment	post-bomb	post-bomb
Site T	2.0	Sediment	1921 (37)	1890
Wetlands	0.9	Sediment	1822 (39)	1790
Wetlands	8.5	Sediment	6309 (53)	7250
Wetlands	8.5	Wood	6195 (68)	7150
Wetlands	15.2	Sediment	7534 (47)	8400
Site A Well[b]	20	DIC	1178	980
Site A Well[b]	51	DIC	986	920

[a] Dates corrected using IntCal04 (Reimer et al., 2004).
[b] Wells adjacent to Site A.

Textural variations within deposited sediments are explained by changing deposition rates and fluvial meandering patterns. Inland wetlands were relatively insulated from channelization by the Mekong River due to the formation of extensive natural levees; annual flooding by levee breaching and monsoonal rains has led to wetland inundation and fine sediment deposition for several thousand years, leaving behind a thick layer of fine sediments. In contrast, old river channels/oxbows have rapidly filled with fine sediments after the Mekong River changed course, and contain a thinner layer of fine sediments near the surface. The ^{14}C dating within the older, thicker fine sediment layer indicates an average deposition rate of ~1–3.3 mm/a over the last 6 ka (from ^{14}C dates measured at depths of 6 and 20 m, Table 1), while Tamura et al. (2007) estimate deposition rates up to ~7 mm/a over the last 0.7 ka (equivalent to ~5 m depth).

4.1.2. General groundwater chemistry

Dissolved As concentrations vary spatially across the aquifer (average: 500 μg/L; range: 15–1300 μg/L) (Table 2, Fig. 2), with the highest dissolved As concentrations observed immediately below (~20 m depth) present-day oxbow channels (Fig. 2). Adjacent to the Mekong River, where aquifer sediments are often coarser than the typical sands, As increases dramatically as a function of depth to >900 μg/L within deep wells (40–57 m). With the exception of the oxbow channel wells and a single well in the center of the interior wetlands, shallow wells (0–13 m) in the field area typically have As concentrations <100 μg/L.

The groundwaters of the site, dominated by Ca^{2+} and HCO_3^-, are representative of those found throughout South and Southeast Asia (Berg et al., 2001; Buschmann et al., 2007; McArthur et al., 2001; Postma et al., 2007). Aquifer groundwaters, shallow well waters (screened in clay), and surface waters are similar yet chemically distinct from one another (Table 2). Average As concentrations are generally the highest in the aquifer and lower in the shallow wells (with the exception of wells installed within wetland and oxbow environments), and lowest (below detection) in surface water samples. Groundwaters have high alkalinities resulting in HCO_3^- providing >70% of the bulk anionic charge in all but five of the wells, while Ca^{2+} is the dominant cation and contributes an average of 46% of the bulk cationic charge. Ammonium concentrations average 20 mg/L and correlate with dissolved organic C which averages 6.9 mg/L. Dissolved organic C and pH are highest in

Table 2
Concentration and ranges of constituents in aqueous samples collected within Kien Svay study site, Kandal, Cambodia

	Aquifer wells ($n = 48$)				Shallow wells ($n = 25$)				Surface water ($n = 24$)			
	Minimum	Maximum	Average	Median	Minimum	Maximum	Average	Median	Minimum	Maximum	Average	Median
As (μg/L)	15	1300	500	480	0.00	1000	160	50	0.0	9.8	1.4	0.0
pH	6.3	9.1	7.1	7.1	6.5	7.4	6.8	6.7	6.2	7.6	6.8	6.8
Eh (mV)	−190	290	70	41	-86	350	110	140	240	450	310	310
TDS (μS/cm)	43	2300	1100	1100	100	3900	1600	1800	11	230	130	130
DO (mg/L)	<1	1.4	<1	<1	<1	2.0	<1	<1	<1	7.5	3.7	3.6
DOC (mg/L)	1.0	24	6.9	5.2	0.09	19	3.3	2.2	2.2	7.1	4.4	4.6
Alkalinity ($CaCO_3$) (mg/L)	200	760	420	420	210	860	530	480	39	96	67	69
Sulfide (μg/L)	<1	96	7.4	2.7	<1	19	2.2	1.0	NA	NA	NA	NA
NH_4–N (mg/L)	1.6	84	20	13	0.75	29	6.4	1.4	0.72	0.88	0.80	0.80
NO_3–N (mg/L)	<0.02	0.08	0.03	0.03	<0.02	15	2.8	0.10	<0.02	0.06	0.01	<0.02
PO_4^{3-} (mg/L)	<0.4	13	3.2	2.7	<0.4	5.6	1.1	<0.4	<0.4	<0.4	<0.4	<0.4
SO_4^{2-} (mg/L)	<0.5	58	8.2	5.6	4.7	440	76	52	0.84	3.8	2.0	2.0
Al (mg/L)	<0.01	0.03	<0.01	<0.01	<0.01	<0.01	<0.01	<0.01	<0.01	0.15	0.03	<0.01
Ca (mg/L)	22	130	71	65	60	290	130	110	11	27	19	19
K (mg/L)	0.88	9.3	3.8	3.2	0.27	36	4.2	1.9	0.20	4.0	1.9	1.8
Fe (mg/L)	0.00	24	8.0	8.0	0.0	26	4.0	2.3	0.0	0.37	0.08	0.04
Mg (mg/L)	8.7	43	24	22	16	120	51	43	2.5	8.1	4.6	4.5
Mn (mg/L)	0.01	3.2	0.79	0.55	0.00	4.9	1.6	1.5	0.00	0.38	0.05	0.03
Na (mg/L)	8.4	110	44	43	12	210	83	74	2.4	8.9	5.7	5.7
P (mg/L)	0.04	4.2	1.2	0.91	0.04	1.9	0.49	0.20	0.00	0.09	0.02	0.02
S (mg/L)	0.47	22	2.4	1.4	1.5	160	28	18	0.59	1.7	0.97	0.99
Si (mg/L)	5.3	37	17	13	7.6	30	16	15	2.3	7.0	5.2	5.4
F^- (mg/L)	<0.3	1.0	<0.3	<0.3	<0.3	1.5	<0.3	<0.3	<0.3	<0.3	<0.3	<0.3
Cl^- (mg/L)	3.5	160	19	9.1	5.2	340	110	58	2.4	9.9	5.9	5.8

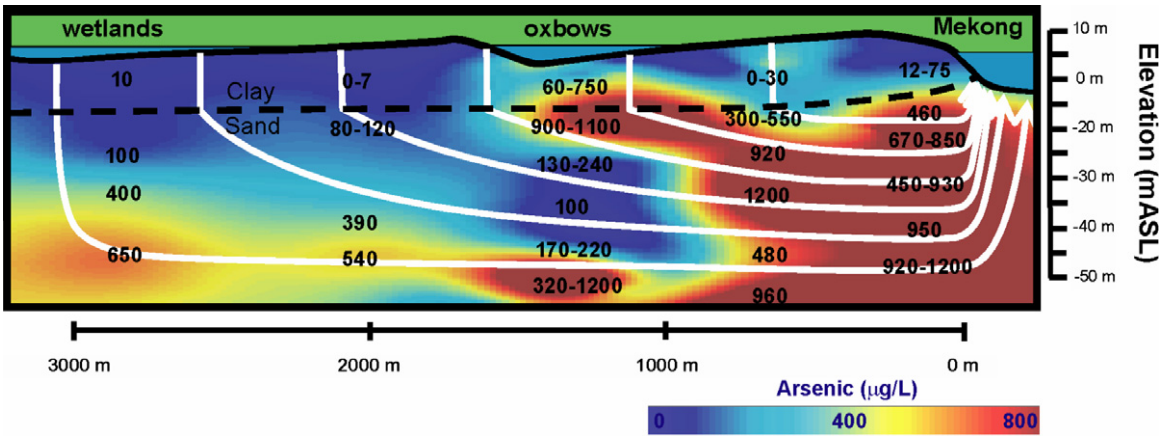

Fig. 2. Field area cross-section (see Fig. 1b) with groundwater As concentrations. Well water As concentrations are depicted with black numbers, and contouring is provided with simple kriging to illustrate As spatial variation. Other than wells adjacent to the oxbow channel ponds, As concentrations in the clay porewater are typically <100 μg/L, while As is >100 μg/L in all but one aquifer sample. Flow-lines are derived in Benner et al. (2008), and the black dotted line represents the clay/sand boundary.

the aquifer groundwater samples and lowest in the shallow wells. Finally, total dissolved solids, alkalinity, Ca^{2+} and Na^{+} are highest in the shallow wells, which may be indicative of evaporative concentration or active weathering in the variable-redox zone.

4.2. Subsurface geochemistry of oxbow channels

4.2.1. Aqueous As concentrations

The profile of As across the field site (Fig. 2) illustrates that differential release occurs within the near-surface in topographic lows that are permanently saturated – the oxbow channels. Accordingly, on the basis of hydrologic flow paths, As released during reductive mobilization within oxbow sediments will be transported downward through the surficial fine sediments (3–20 m) and then horizontally toward the Mekong River. The examination is therefore focused on biogeochemical processes, and factors influencing them, within this area of the floodplain.

Groundwater As concentrations within the oxbow channel area increased nearly linearly as a function of depth (Fig. 3, Site T wells in blowup of Fig. 1b), from 0 to 15 μg/L at 2 m to more than 200–600 μg/L at 7 m. Lysimeter-collected pore-water As concentrations were greater than 10 μg/L at 10 cm, and increased to approximately 100 μg/L at 4 m at site T, and over 200 μg/L at site A. Seasonal As variation was not observed at site T, and water level measurements from wells screened at different depths indicated a consistent downward hydraulic gradient. However, seasonal variation was observed within porewaters collected from site A, with high As concentrations also observed coincident with the development of a steep downward hydraulic gradient, indicating As is likely flushed to the deeper subsurface during monsoonal flooding (Polizzotto et al., 2008).

A strong correlation generally exists between As and dissolved Fe and alkalinity (as HCO_3^-) within porewaters (Fig. 4). This correlation is the most consistent below the lowest annual position of the water table of approximately 1–2 m below the surface, where sediment color transitions from red (oxidized Fe) to gray (comparatively reduced). Above this depth, As concentrations are more weakly correlated with Fe and alkalinity, although dissolved Fe and alkalinity still represent appreciable solution constituents. Increases in DOC and DIC concentrations as a function of depth support As liberation via anaerobic microbial respiration in the near-surface (Fig. 3); DIC concentrations increase from 50 mg/L in the surface waters (Table 2) to >1000 mg/L at 6–8 m depth (Fig. 3). Moreover, the DIC is much younger (<1.0 ka, Table 1) than the age of the aquifer (>6 ka) and must, therefore be derived from a more recent (i.e., surface) organic C source. The sum of all respiratory processes contributing HCO_3^- to solution will enhance the competitive ligand sorption effect with As (Appelo et al., 2002; Stachowicz et al., 2007), although the magnitude of the effect is likely small relative to reductive dissolution (Radu et al., 2005).

Arsenic is not correlated with SO_4^{2-}; low As concentrations are observed in the presence of high (30 mg/L) SO_4^{2-} from porewaters collected at 10 cm, compared to porewaters deeper than 50 cm (Fig. 3), where As concentrations are higher and SO_4^{2-} is absent. Finally, dissolved Si, derived from silicate-bearing mineral weathering or liberation from Si-substituted Fe (hydr)oxides, increases with As at lower concentrations. Within all oxbow channel groundwater samples, aqueous silicon is relatively high (average concentration ~15–20 mg/L), and oversaturated with respect to quartz, and may compete with As for adsorption sites (Luxton et al., 2006).

4.2.2. Total and extractable arsenic within soils/sediments

Total solid-phase As was analyzed from sediments collected throughout the focused oxbow channel area during well installation (Fig. 5), and generally decreases as a function of depth. Samples collected from the red clay (0–2 m) range in concentration from 6 to 13 mg/L, while samples below the seasonal water table (within gray sediments)

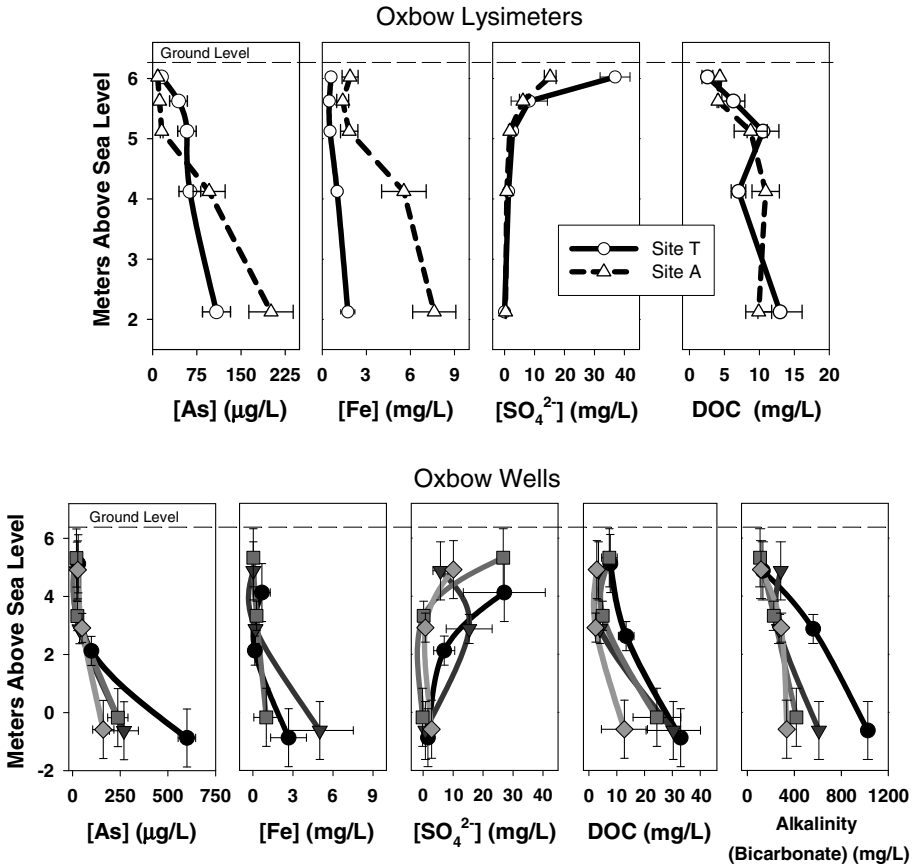

Fig. 3. Arsenic, Fe, SO_4^{2-} and DOC from lysimeters (Site A and T) installed within oxbow sediments (top), and As, Fe, SO_4^{2-}, DOC and alkalinity from well nests (2, 4 and 8 m depths) installed within the oxbow study area (see Fig. 1b, blowup).

have relatively less As, and range from 2 to 5 mg/kg at 7 m depth.

Within a set of samples collected at site A for selective extractions, total solid-phase As concentrations 0–4 m below the oxbow channel ponds were approximately 12 mg/kg (Fig. 6). No resolvable trends were apparent as a function of depth for salt-exchangeable extractions, which yielded ~0–3 mg/kg As (Fig. 6). Acid extractable treatments, which tend to remove amorphous phases including those of Fe (hydr)oxides, yielded 3–6 mg/kg As, and increased slightly as a function of depth (Fig. 6). Citrate–bicarbonate–dithionate extractable As (targeting As associated with reducible Fe and Mn phases, hereafter referred to as the Fe-reducible fraction) represented 6–14 mg/kg As, and phosphate-extractable As represented 6–9 mg/kg throughout the profile (Fig. 6). Thus, the Fe-reducible fraction yielded As concentrations approximating total extractable As, although below 1 m they differ from total As value by ~5 mg/kg and above 1 m they are higher by ~2–9 mg/kg. Slightly higher concentrations of As were recovered between 0.1–2 m (within the red clay) for Fe-reducible and total extractions (Fig. 6) relative to gray solids collected below the seasonal water table (~2 m), similar to the trend of decreasing total As found within the large set of extractions performed from sediments throughout the oxbow channel (Fig. 5).

Although typical solid-phase As concentrations are below limits required for bulk speciation techniques, micro-X-ray absorption near-edge structure (µ-XANES) spectroscopy was used to determine As speciation within the sediments (Fig. 7). In the upper surface sediments (10 cm), As exists predominantly as arsenate, but with increasing depth (1–4 m), arsenite dominates the solid-phase speciation. Additionally, the deeper reduced sediments (4 m and greater) also contain As-bearing sulfide grains. Such varying As speciation demonstrates active redox processes involving As at the near-surface (0–4 m), with As becoming increasingly reduced as a function of depth.

5. Discussion

Within the aqueous phase, there is a steep gradient in As concentrations downwards in near-surface soil/sediment pore water from <50 µg/L at 10 cm below the surface (Fig. 3), to concentrations >100 µg/L at a depth of 4 m below the surface, increasing to >600 µg/L at 7 m depth (~−1 MASL). In order to identify the desorption/dissolu-

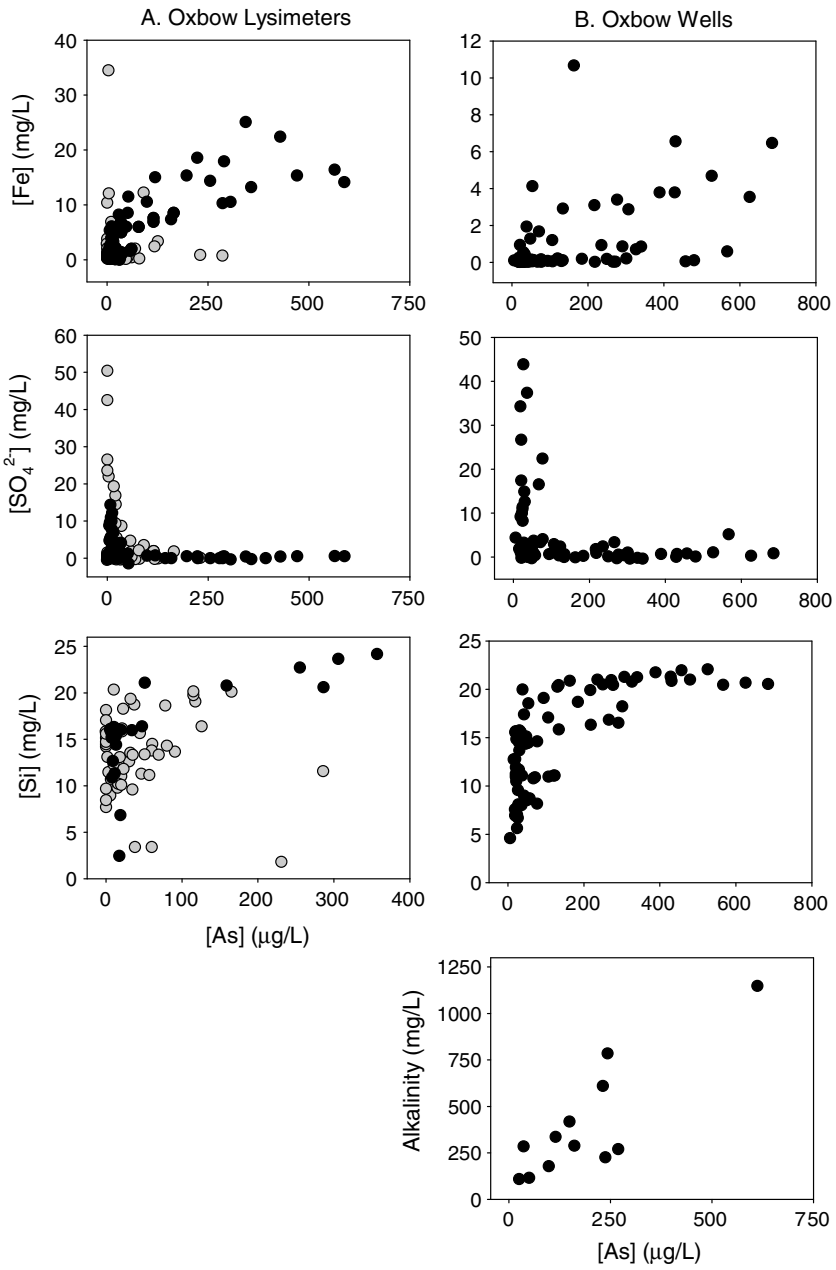

Fig. 4. (A) Correlation plots for As with Fe, S and Si within porewater collected from lysimeters (0.1, 0.5, 1, 2 and 4 m depth). Gray fills are site T lysimeter porewaters, black fills are site A porewaters. (B) Correlation plots for As with Fe, S, Si, and alkalinity from well samples collected within the oxbow study area (Fig. 1b).

tion mechanisms responsible for this sharp As gradient, the (bio)geochemical conditions within the sediment system must be deciphered from the sediment source and then along the hydrologic flow path.

Arsenic in the sedimentary basins of Asia originates from the Himalayas. Arsenic-bearing rocks erode and weather to As-bearing Fe (hydr)oxides, which are transported and deposited, along with residual primary mineral sources, by fluvial systems within vast Holocene sediments of the large deltas. Within these deposits, appreciable fractions of As remain adsorbed on labile Fe (hydr)oxide phases; As is thus prone to release during As and Fe reduction, processes fueled by the degradation of particulate and/or dissolved organic matter.

The data illustrate that the highest concentrations of dissolved As within the aquifer originate from recent sediments deposited within oxbow channels (Fig. 2), where As concentrations increase linearly with depth from the surface to the fine sediment/sand interface at ~12 m, and where abundant DOC is available to drive biogeochemical

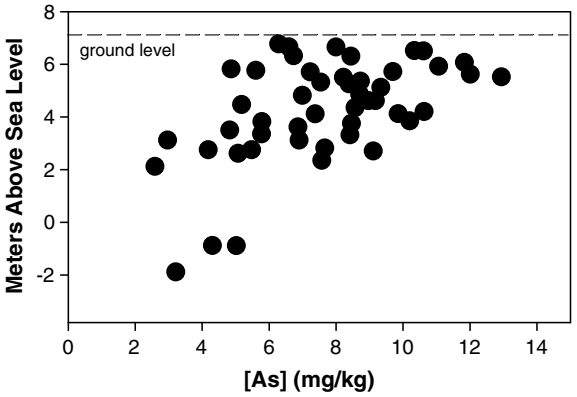

Fig. 5. Total As concentration in sediments collected within oxbow channel focused study site (Fig. 1b).

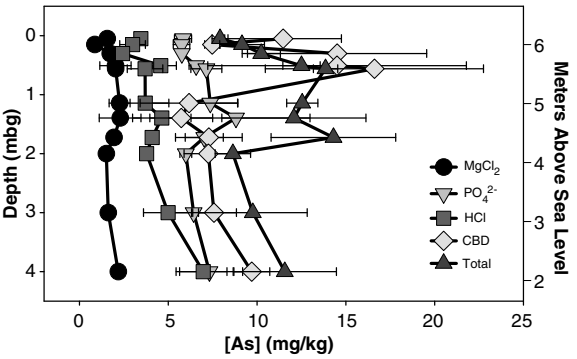

Fig. 6. Selective extractions of oxbow sediments as a function of depth. Triplicate samples were collected at each depth from three separate boreholes. Error bars represent standard deviation of triplicate analyses.

reactions (Fig. 3). Oxbow channels form after river diversion from a historic channel, and receive yearly sediment deposition during annual flooding. This occurs owing to the low topography of the channels (and other low-lying wetland areas) compared to historic natural levees, which may rise 2 or more meters higher. During the prolonged flooding stage of these surficial features, high primary productivity and decomposition of organic matter maintain reducing conditions, and provide sufficient input of particulate organic C during sedimentation to induce long-term Fe and As reduction (Fig. 8). Even during the dry season, water levels within shallow wells do not recede more than ~1–2 m below the surface, leading to a dominance of anaerobic conditions within the shallow sediments. As a consequence, reductive mobilization of As will commence in the near-surface after deposition and continue with depth during burial until either labile As is depleted or the dissolution reactions cease due to exhaustion of labile C.

Within the oxbow soils/sediments, dissolved As is regularly detected at concentrations of 10–50 μg/L within porewaters at depths of only 10 cm. At this depth, soils are young (<500 a old) and are variably saturated. Under conditions of continued re-wetting and drying, Fe (hydr)oxides may transform to more stable, lower surface area minerals (Thompson et al., 2006), likely releasing small quantities of As. At depths of ~1 m, soils retain characteristic red hues indicative of ferric (hydr)oxides, although they are maintained in a nearly permanent saturated state. However, Fe reduction is clearly occurring as noted by increasing Fe(II) concentrations (Fig. 3), and As may be released both through reductive dissolution of Fe and reduction of As(V) to As(III) (Fig. 8).

Progressing below the seasonal water table (~2 m depth), continuous anaerobic conditions (highly reducing, as measured by the presence of reduced species – NH_4^+, Fe^{2+} and S(-II) – and low Eh measurements) resulting in extensive Fe and As reduction lead to increased release of As relative to transiently saturated conditions above. Ferric (hydr)oxide dissolution coupled with Fe(II) induced surface destabilization (Larese-Casanova and Scherer, 2007), along with conversion of As(V) to As(III), results in extensive As desorption (McArthur et al., 2004), as evidenced by a measurable fraction of salt-exchangeable As within

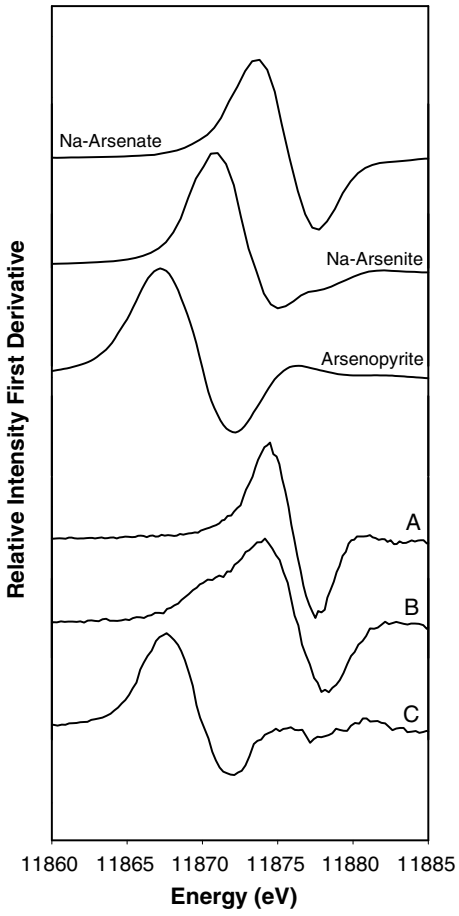

Fig. 7. First-derivative μ-XANES of near-surface sediments from site adjacent to oxbow ponds. (A) Sediments at 10 cm depth show As predominantly as arsenate (As(V)). (B) Sediments at 4 m depth show a mixture of arsenite (As(III)) and arsenate (As(V)). (C) In 4 m sediments, As is also found associated with sulfides in individual sediment As "hotspots".

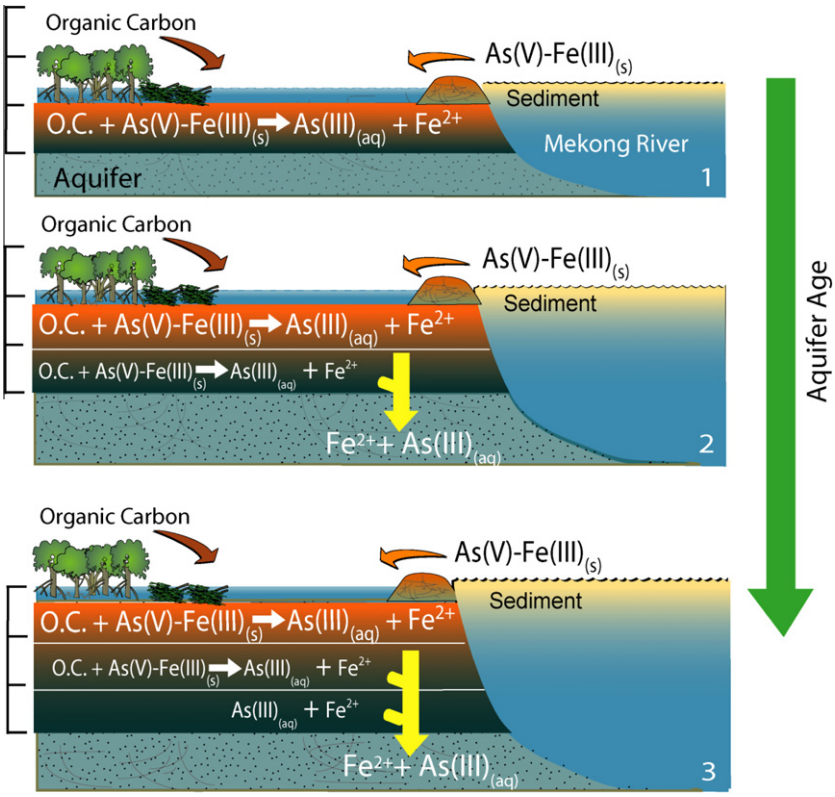

Fig. 8. Conceptual diagram of As-bearing sediment deposition within the wetland floodplain environment. Scale bars (left side) are used as a reference for sediment burial and represent arbitrary lengths. Influx of organic matter to saturated As-bearing sediment induces As(V) and Fe(III) reduction, with subsequent As liberation to pore-water (1). Continued influx of OM and As-sediment to anaerobic soil results in As release. Dissolved As is then subject to downward transport. Arsenic liberation, via As(V) and Fe(III) reduction, progresses with depth/time until Fe oxides or organic C is exhausted (2). Exhaustion of Fe(III) and OM removes in-situ source; dissolved As concentrations are maintained by limited elution or surficial influx of As (3).

the solid phase (Fig. 6). As the sediments are buried deeper with time, the ferric (hydr)oxides are depleted through continued Fe reduction, resulting in further (and continuous) release of As (Fig. 8), represented by the fraction of As released during acid and Fe-reducible extraction (Fig. 6). Although likely smaller in magnitude, silicate, bicarbonate and other microbial metabolites will further enhance desorption of As(III) from existing mineral surfaces (Appelo et al., 2002; Luxton et al., 2006).

Sulfate reduction is also a prominent process, as evidenced by increasing S(-II) (Table 2) and decreasing SO_4^{2-} (Fig. 3) in sediment porewaters. Thus, in addition to direct enzymatic reduction, Fe (hydr)oxides may also be degraded by sulfide attack (Poulton et al., 2004). Deeper within the aquifer, labile Fe oxides are largely absent and As, as As(III), reaches a maximum concentration in the aqueous phase (McArthur et al., 2004) that may persist along groundwater flowpaths (Harvey et al., 2002). While varying spatially, sulfide (and, through a combination of reactions, disulfide) generated from SO_4^{2-} (or organic S) reduction, combined with Fe(II), leads to the formation of pyritic materials, as found within deeper sediments (Fig. 7). Arsenic(III) and/or As_x-$(SH)_x$ intermediates (Wilkin et al., 2003) associated with Fe–S surfaces (Bostick and Fendorf, 2003) can incorporate As, representing a potential sink of As within very reducing sediments (Lowers et al., 2007).

During sediment burial from continued deposition, As will progressively be released via reductive mobilization until, finally, either labile organic matter or As-bearing Fe (hydr)oxides are exhausted; release rates will, however, be most rapid when Fe (hydr)oxides are nearly consumed and sorption capacity is thereby depleted (Herbel and Fendorf, 2006; Kocar et al., 2006) – this appears to be the case ~3–4 m below oxbow ponds, where sediment color transitions from red to gray and where less As is associated with the solid phase (Fig. 5). Additionally, co-buried Fe (hydr)oxides and organic C will be the most reactive immediately following exposure to continuously reducing conditions (e.g. conditions are immediately thermodynamically favorable for As and Fe reduction), and As release will therefore proceed early in the depositional history (i.e. within the near-surface) if sediments are deposited in flooded surface environments. Thus, if a 'sediment packet' (an artificial lumping of sediment during some deposition period) is considered, As will be released most extensively below the seasonal water table (~2 m), and release will progress at decreasing rates with increasing depth until liberation finally ceases deep in the aquifer (shown schematically in Fig. 8) where Fe-(hydr)oxides are depleted. Stimulated

release of As from deeply buried Fe (hydr)oxides is unlikely since these sediments did not contain sufficient organic C to drive Fe reduction preceding burial near the surface. Arsenic in the deep portions of the aquifer therefore would result from either 'old' water (i.e. stagnant porewater still remaining from the initial stages of surface deposition and release of As) and/or the influx of As with recharging waters.

6. Summary and conclusions

A steep vertical gradient in As concentration is observed within wetland environments studied in the field site, with detectable concentrations found within very shallow sediment porewaters (10 cm) and increasing to >600 μg/L at 7 m BGL. These locations are seasonally inundated during monsoonal flooding, which delivers As through sedimentation and provides fresh organic C from extensive growth and decomposition of aquatic plant material. Degradation of organic matter within these environment drives reductive dissolution of Fe (hydr)oxides and reduces As(V) to As(III), releasing As to porewater within the upper 0–12 m of sediment.

In a companion article (Benner et al., 2008), hydrologic modeling calibrated with extensive field data demonstrates that subsurface flow is dictated by monsoonal flooding, where the net annual subsurface flow extends from the floodplain environment (inclusive of the wetlands) to the Mekong River (Fig. 2 and Benner et al., 2008). Importantly, the companion paper demonstrates that a net annual downward flow exists within the near-surface clays (0–12 m), where active As solubilization is observed (Fig. 3). Therefore, sustained cycles of As-bearing sediment deposition during monsoonal flooding, near-surface reductively mediated As solubilization, and subsequent downward transport to the aquifer results in extensive and continuous release to groundwaters. Although deeper sources of As (e.g. buried As-bearing Fe (hydr)oxides) may contribute As to the subsurface environment, the observations highlight that the synthesis of near-surface biogeochemical and hydraulic processes result in extensive As contamination of underlying aquifers.

Acknowledgements

This work was supported by 3 US EPA STAR graduate fellowships and the Stanford NSF Environmental Molecular Sciences Institute (NSF-CHE-0431425). We are grateful to Guangchao Li for helpful discussion and laboratory assistance. We are indebted to Matthew Newville (APS-GSE-CARS) for his assistance with XAS data collection and analysis. Portions of this work were performed at GeoSoilEnviroCARS (Sector 13), Advanced Photon Source (APS), Argonne National Laboratory, supported by the National Science Foundation – Earth Sciences (EAR-0217473), Department of Energy – Geosciences (DE-FG02-94.ER14466), and the State of Illinois under the US Department of Energy, Office of Science, Office of Basic Energy Sciences, Contract No. W-31-109.-ENG-38.

References

Ahmed, K.M., Bhattacharya, P., Hasan, M.A., Akhter, S.H., Alam, S.M.M., Bhuyian, M.A.H., Imam, M.B., Khan, A.A., Sracek, O., 2004. Arsenic enrichment in groundwater of the alluvial aquifers in Bangladesh: an overview. Appl. Geochem. 19, 181–200.

Ahmed, M.F., Ahuja, S., Alauddin, M., Hug, S.J., Lloyd, J.R., Pfaff, A., Pichler, T., Saltikov, C., Stute, M., van Geen, A., 2006. Epidemiology – ensuring safe drinking water in Bangladesh. Science 314, 1687–1688.

Akai, J., Izumi, K., Fukuhara, H., Masuda, H., Nakano, S., Yoshimura, T., Ohfuji, H., Anawar, H.M., Akai, K., 2004. Mineralogical and geomicrobiological investigations on groundwater arsenic enrichment in Bangladesh. Appl. Geochem. 19, 215–230.

Anawar, H.M., Akai, J., Komaki, K., Terao, H., Yoshioka, T., Ishizuka, T., Safiullah, S., Kato, K., 2003. Geochemical occurrence of arsenic in groundwater of Bangladesh: sources and mobilization processes. J. Geochem. Explor. 77, 109–131.

Appelo, C.A.J., Van der Weiden, M.J.J., Tournassat, C., Charlet, L., 2002. Surface complexation of ferrous iron and carbonate on ferrihydrite and the mobilization of arsenic. Environ. Sci. Technol. 36, 3096–3103.

Benner, S.G., Polizzotto, M.L., Kocar, B.D., Sampson, M., Fendorf, M., 2008. Groundwater flow in an arsenic-contaminated aquifer, Mekong Delta, Cambodia. Appl. Geochem. 23 (11), 3072–3087.

Berg, M., Tran, H.C., Nguyen, T.C., Pham, H.V., Schertenleib, R., Giger, W., 2001. Arsenic contamination of groundwater and drinking water in Vietnam: a human health threat. Environ. Sci. Technol. 35, 2621–2626.

Berg, M., Stengel, C., Trang, P.T.K., Viet, P.H., Sampson, M.L., Leng, M., Samreth, S., Fredericks, D., 2007. Magnitude of arsenic pollution in the Mekong and Red River Deltas – Cambodia and Vietnam. Sci. Total Environ. 372, 413–425.

Bostick, B.C., Fendorf, S., 2003. Arsenite sorption on troilite (FeS) and pyrite (FeS_2). Geochim. Cosmochim. Acta 67, 909–921.

Buschmann, J., Berg, M., Stengel, C., Sampson, M.L., 2007. Arsenic and manganese contamination of drinking water resources in Cambodia: coincidence of risk areas with low relief topography. Environ. Sci. Technol. 41, 2146–2152.

Chakraborti, D., Rahman, M.M., Paul, K., Chowdhury, U.K., Sengupta, M.K., Lodh, D., Chanda, C.R., Saha, K.C., Mukherjee, S.C., 2002. Arsenic calamity in the Indian subcontinent – what lessons have been learned? Talanta 58, 3–22.

deLemos, J.L., Bostick, B.C., Renshaw, C.E., Sturup, S., Feng, X.H., 2006. Landfill-stimulated iron reduction and arsenic release at the Coakley Superfund Site (NH). Environ. Sci. Technol. 40, 67–73.

Dowling, C.B., Poreda, R.J., Basu, A.R., Peters, S.L., Aggarwal, P.K., 2002. Geochemical study of arsenic release mechanisms in the Bengal Basin groundwater. Water Resour. Res. 38, 1173.

GLCF, 2005. Global Land Cover Facility. University of Maryland, <http://www.landcover.org>.

Harvey, C.F., Swartz, C.H., Badruzzaman, A.B.M., Keon-Blute, N., Yu, W., Ali, M.A., Jay, J., Beckie, R., Niedan, V., Brabander, D., Oates, P.M., Ashfaque, K.N., Islam, S., Hemond, H.F., Ahmed, M.F., 2002. Arsenic mobility and groundwater extraction in Bangladesh. Science 298, 1602–1606.

Harvey, C.F., Ashfaque, K.N., Yu, W., Badruzzaman, A.B.M., Ali, M.A., Oates, P.M., Michael, H.A., Neumann, R.B., Beckie, R., Islam, S., Ahmed, M.F., 2006. Groundwater dynamics and arsenic contamination in Bangladesh. Chem. Geol. 228, 112–136.

Herbel, M., Fendorf, S., 2006. Biogeochemical processes controlling the speciation and transport of arsenic within iron coated sands. Chem. Geol. 228, 16–32.

Islam, F.S., Gault, A.G., Boothman, C., Polya, D.A., Charnock, J.M., Chatterjee, D., Lloyd, J.R., 2004. Role of metal-reducing bacteria in arsenic release from Bengal delta sediments. Nature 430, 68–71.

JICA, 2002. The study on groundwater development in southern Cambodia. Draft Report by Kokusai Kogyo Co. Ltd. to the Ministry of Rural Development, Phnom Penh, Cambodia.

Keon, N.E., Swartz, C.H., Brabander, D.J., Harvey, C., Hemond, H.F., 2001. Validation of an arsenic sequential extraction method for evaluating mobility in sediments. Environ. Sci. Technol. 35, 2778–2784.

Kinniburgh, D.G., Smedley, P.L., 2001. Arsenic contamination of groundwater in Bangladesh. In: BGS and DPHE, Report WC/00/19. Keyworth, England.

Kocar, B.D., Herbel, M.J., Tufano, K.J., Fendorf, S., 2006. Contrasting effects of dissimilatory iron(III) and arsenic(V) reduction on arsenic retention and transport. Environ. Sci. Technol. 40, 6715–6721.

Larese-Casanova, P., Scherer, M.M., 2007. Fe(II) sorption on hematite: New insights based on spectroscopic measurements. Environ. Sci. Technol. 41, 471–477.

Loeppert, R.H., Inskeep, W.P., 1996. Iron. In: Bigham, J.M. (Ed.), Methods of Soil Analysis. Soil Science Society of America, Inc., Madison, pp. 639–664.

Lowers, H.A., Breit, G.N., Foster, A.L., Whitney, J., Yount, J., Uddin, Md.N., Muneem, Ad.A., 2007. Arsenic incorporation into authigenic pyrite, Bengal Basin sediment, Bangladesh. Geochim. Cosmochim. Acta 71, 2699–2717.

Luxton, T.P., Tadanier, C.J., Eick, M.J., 2006. Mobilization of arsenite by competitive interaction with silicic acid. Soil Sci. Soc. Am. J. 70, 204–214.

Masscheleyn, P.H., Delaune, R.D., Patrick, W.H., 1991. A hydride generation atomic-absorption technique for arsenic speciation. J. Environ. Qual. 20, 96–100.

McArthur, J.M., Ravenscroft, P., Safiulla, S., Thirlwall, M.F., 2001. Arsenic in groundwater: testing pollution mechanisms for sedimentary aquifers in Bangladesh. Water Resour. Res. 37, 109–117.

McArthur, J.M., Banerjee, D.M., Hudson-Edwards, K.A., Mishra, R., Purohit, R., Ravenscroft, P., Cronin, A., Howarth, R.J., Chatterjee, A., Talukder, T., Lowry, D., Houghton, S., Chadha, D.K., 2004. Natural organic matter in sedimentary basins and its relation to arsenic in anoxic ground water: the example of West Bengal and its worldwide implications. Appl. Geochem. 19, 1255–1293.

Nguyen, V.L., Ta, T.K.O., Tateishi, M., 2000. Late Holocene depositional environments and coastal evolution of the Mekong River Delta, Southern Vietnam. J. Asian Earth Sci. 18, 427–439.

Nickson, R., McArthur, J., Burgess, W., Ahmed, K.M., Ravenscroft, P., Rahman, M., 1998. Arsenic poisoning of Bangladesh groundwater. Nature 395, 338.

Nordstrom, D.K., 2002. Public health – worldwide occurrences of arsenic in ground water. Science 296, 2143–2145.

Polizzotto, M.L., Harvey, C.F., Sutton, S.R., Fendorf, S., 2005. Processes conducive to the release and transport of arsenic into aquifers of Bangladesh. PNAS 102, 18819–18823.

Polizzotto, M.L., Kocar, B.D., Benner, S.B., Sampson, M., Fendorf, S., 2008. Near-surface wetland sediments as a source of arsenic release to ground water in Asia. Nature 454, 505–508.

Polya, D.A., Lythgoe, P.R., Abou-Shakra, F., Gault, A.G., Brydie, J.R., Webster, J.G., Brown, K.L., Nimfopoulos, M.K., Michailidis, K.M., 2003. IC-ICP-MS and IC-ICP-HEX-MS determination of arsenic speciation in surface and ground waters: preservation and analytical issues. Miner Mag. 67, 247–261.

Polya, D.A., Gault, A.G., Diebe, N., Feldman, P., Rosenboom, J.W., Gilligan, E., Fredericks, D., Milton, A.H., Sampson, M., Rowland, H.A.L., Lythgoe, P.R., Jones, J.C., Middleton, C., Cooke, D.A., 2005. Arsenic hazard in shallow Cambodian groundwaters. Mineral Mag. 69, 807–823.

Postma, D., Larsen, F., Hue, N.T.M., Duc, M.T., Viet, P.H., Nhan, P.Q., Jessen, S., 2007. Arsenic in groundwater of the Red River floodplain, Vietnam: controlling geochemical processes and reactive transport modeling. Geochim. Cosmochim. Acta 71, 5054–5071.

Poulton, S.W., Krom, M.D., Raiswell, R., 2004. A revised scheme for the reactivity of iron (oxyhydr)oxide minerals towards dissolved sulfide. Geochim. Cosmochim. Acta 68, 3703–3715.

Radu, T., Subacz, J.L., Phillippi, J.M., Barnett, M.O., 2005. Effects of dissolved carbonate on arsenic adsorption and mobility. Environ. Sci. Technol. 39, 7875–7882.

Reimer, P.J., Baillie, M.G.L., Bard, E., Bayliss, A., Beck, J.W., Bertrand, C.J.H., Blackwell, P.G., Buck, C.E., Burr, G.S., Cutler, K.B., Damon, P.E., Edwards, R.L., Fairbanks, R.G., Friedrich, M., Guilderson, T.P., Hogg, A.G., Hughen, K.A., Kromer, B., McCormac, G., Manning, S., Ramsey, C.B., Reimer, R.W., Remmele, S., Southon, J.R., Stuiver, M., Talamo, S., Taylor, F.W., van der Plicht, J., Weyhenmeyer, C.E., 2004. IntCal04 terrestrial radiocarbon age calibration, 0–26 cal kyr BP. Radiocarbon 46, 1029–1058.

Smedley, P.L., Kinniburgh, D.G., 2002. A review of the source, behaviour and distribution of arsenic in natural waters. Appl. Geochem. 17, 517–568.

Stachowicz, M., Hiemstra, T., Van Riemsdijk, W.H., 2007. Arsenic-bicarbonate interaction on goethite particles. Environ. Sci. Technol. 41, 5620–5625.

Stanger, G., VanTruong, T., Ngoc, K., Luyen, T.V., Thanh, T.T., 2005. Arsenic in groundwaters of the Lower Mekong. Environ. Geochem. Health 27, 341–357.

Ta, T.K.O., Nguyen, V.L., Tateishi, M., Kobayashi, I., Tanabe, S., Saito, Y., 2002. Holocene delta evolution and sediment discharge of the Mekong River southern Vietnam. Quatern. Sci. Rev. 21, 1807–1819.

Tamura, T., Saito, Y., Sieng, S., Ben, B., Kong, M., Choup, S., Tsukawaki, S., 2007. Depositional facies and radiocarbon ages of a drill core from the Mekong River lowland near Phnom Penh, Cambodia: evidence for tidal sedimentation at the time of Holocene maximum flooding. J. Asian Earth Sci. 29, 585–592.

Thompson, A., Chadwick, O.A., Rancourt, D.G., Chorover, J., 2006. Iron-oxide crystallinity increases during soil redox oscillations. Geochim. Cosmochim. Acta 70, 1710–1727.

van Geen, A., Zheng, Y., Versteeg, R., Stute, M., Horneman, A., Dhar, R., Steckler, M., Gelman, A., Small, C., Ahsan, H., Graziano, J.H., Hussain, I., Ahmed, K.M., 2003. Spatial variability of arsenic in 6000 tube wells in a 25 km^2 area of Bangladesh. Water Resour. Res. 39, 1140. doi:10.1029/2002WR00161.

Wilkin, R.T., Wallschlager, D., Ford, R.G., 2003. Speciation of arsenic in sulfidic waters. Geochem. Trans. 4, 1–7.

Wolf, D.C., Dao, T.H., Scott, H.D., Lavy, T.L., 1989. Influence of sterilization methods on selected soil microbiological, physical, and chemical properties. J. Environ. Qual. 18, 39–44.

Yu, W.H., Harvey, C.M., Harvey, C.F., 2003. Arsenic in groundwater in Bangladesh: a geostatistical and epidemiological framework for evaluating health effects and potential remedies. Water Resour. Res. 39, 1–17.